Space-time evolution of a decaying quantum state

1999 J. Phys. A: Math. Gen. 32 6347

(http://iopscience.iop.org/0305-4470/32/35/311)

J. Phys. A: Math. Gen. **32** (1999) 6347–6360. Printed in the UK PII: S0305-4470(99)02094-6

Space-time evolution of a decaying quantum state

W van Dijk†‡, F Kataoka‡ and Y Nogami‡

† Redeemer College, Ancaster, Ontario, Canada L9K 1J4
‡ Department of Physics and Astronomy, McMaster University, Hamilton, Ontario, Canada L8S 4M1

E-mail: vandijk@physics.mcmaster.ca

Received 24 February 1999, in final form 9 July 1999

Abstract. We examine a one-dimensional model of a decaying quantum system, e.g., one that could simulate α decay. A particle is initially confined in a region and leaks out, tunnelling through a potential barrier. The same model has been examined before, primarily to study decay properties which are determined by the wavefunction of the particle within the potential barrier. However, the wavefunction of this model (and of any similar models) outside the potential barrier has not been obtained explicitly as a function of position and time. We obtain the wavefunction outside as well as inside the potential barrier by solving the time-dependent Schrödinger equation, and explore various features of the space-time development of the system. In an early study by Winter it was pointed out that the probability current just outside the barrier, after a long time, may fluctuate and can be negative, i.e., inward. We find that under certain circumstances the amplitude of the fluctuations increases significantly as the distance from the barrier increases. We propose a simple approximate wavefunction that works well when the decay is very slow. The Gamow wavefunction, commonly used to describe the α-decay process, is not appropriate at large distances. Our wavefunction can be used anywhere and is normalized in the usual manner.

1. Introduction

The evolution of a decaying quantum state is one of the oldest problems in quantum mechanics. As a typical case let us consider the decay of a quantum system of the type initiated by Gamow [1] and by Condon and Gurney [2]. The model assumes that a particle is initially confined and at a certain time, $t = 0$, it begins to leak out by tunnelling through a potential barrier. The model has been studied extensively and various ingenious methods have been developed. The model is successful in explaining the exponential decay law which has ample experimental support. More detailed scrutiny revealed interesting deviations from the exponential law for very small t as well as for very large t. We still feel, however, that our understanding of the decay problem is far less than complete. This is because, as far as we know, the wavefunction of the particle of the model over the entire space has not been worked out explicitly as a function of position and time. All work done so far on the decaying state focused on the wavefunction at and inside the potential barrier, and very little is known about the behaviour of the wavefunction outside the potential barrier. The so-called Gamow state or Gamow wavefunction is often used [1, 3]. The Gamow wavefunction, however, increases exponentially in magnitude at large distances. Therefore, despite its merits for determining α-particle decay rates, etc, the Gamow wavefunction is not a desirable wavefunction over all space because it is not square integrable. This difficulty stems from the fact that, in the Gamow wavefunction, the initial condition that the decay process begins at $t = 0$ is not fully taken into

0305-4470/99/356347+14$30.00

account [4]. The main purpose of this paper is to find the correct wavefunction at all distances by explicitly solving the time-dependent Schrödinger equation.

A problem in which such a time-dependent wavefunction at large distances is needed is the quantum mechanical treatment of atomic ionization caused by α decay of the nucleus. Traditionally this ionization problem has been treated, after Migdal, by regarding the emitted α particle as a point charge that obeys Newton's equation of classical mechanics [5, 6]. In a fully quantum mechanical calculation, the α particle should be treated as a wave that leaks out of the nucleus. We are aware of only one calculation in which the α particle is treated quantum mechanically [7]. In that calculation, however, the α particle is described by means of a quasi-stationary state with complex energy. Since α decay is an intrinsically time-dependent phenomenon, the validity of such quasi-stationary treatment is not entirely obvious. In this paper we focus on the decay process itself but in a forthcoming paper we plan a fully quantum mechanical calculation for a model that simulates the atomic ionization process. In order to do such a calculation we have to be able to first solve the time-dependent Schrödinger equation for a decaying system.

Instead of a detailed realistic calculation we consider a simple one-dimensional model. This is the same model that has been examined by a number of people, in particular, by Petzold [8] and Winter [9], and more recently by García-Calderón *et al* [10–12]. Although simple, the model illustrates many interesting features as well as difficulties that are characteristic of the decay process in quantum mechanics. The model consists of a particle which is subject to an infinite repulsive wall at $x = -a$ and a repulsive barrier represented by a δ-function potential at $x = 0$. The particle is initially confined in the region of $-a < x < 0$ and begins to leak out at $t = 0$ tunnelling through the barrier. As shown by Petzold [8], by Winter in more detail [9] and also by García-Calderón *et al* [10–12], the time-dependent wavefunction $\psi(x, t)$ can be expressed in the form of an integral with an integrand that can be written down explicitly. The integrand, however, is highly oscillatory with large amplitude. It is difficult to carry out the integration numerically except for small values of x. Probably for this reason, $\psi(x, t)$ of the model has not been obtained explicitly outside the barrier, $x > 0$.

Of course, the wavefunction inside the potential barrier contains a significant amount of information on the decay process. Winter examined $\psi(0, t)$ and the associated current $j(0, t)$ at the barrier. He illustrated small deviations from the exponential decay law for extremely small t and extremely large t. A particularly remarkable and curious feature that he found is that $j(0, t)$ fluctuates as a function of t in a certain large t region. It can be negative, meaning that the current can flow inward. It would be interesting to see how $j(x, t)$ behaves for $x > 0$.

In section 2 we set up the model and briefly summarize some of Winter's results. We then extend Winter's calculation by carrying out the integral for $\psi(x, t)$ for larger values of x. We have been able to do this only to a certain limit. We discuss the nature of the difficulty that is encountered. We show that the amplitude of fluctuations that Winter found for $j(0, t)$ becomes much larger as x increases. In section 3 we integrate the time-dependent Schrödinger equation numerically and obtain $\psi(x, t)$ in the entire space. In section 4 we propose a simple approximate wavefunction that works well when the decay process is very slow. The conclusion and a discussion are given in section 5. The appendix enlarges on the negative local current density which is present in the model.

2. Model

Consider a one-dimensional, non-relativistic model, with a particle of mass m in a potential that consists of an infinite repulsive wall at $x = -a$ and a repulsive δ-function potential at

$x = 0$ [8–12],

$$V(x) = \begin{cases} \infty & x < -a \\ (g/2m)\delta(x) & x \geqslant -a \end{cases} \tag{1}$$

where $a > 0$ and $g > 0$. We use units such that $\hbar = 1$, throughout. In numerical illustrations, we further set $a = 1$ and $2m = 1$. Let us follow Winter's elementary approach rather than the Laplace transform method used in [8, 10–12].

Since $V(x)$ has no attractive part, there is no bound state. The spatial part of the wavefunction of the stationary continuum state of energy $E = k^2/2m$ can be written as

$$\phi_k(x) = \begin{cases} \dfrac{1}{\sqrt{\pi}} \dfrac{\sin(ka + \delta_k)\sin k(x + a)}{\sin ka} & -a < x < 0 \\ \dfrac{1}{\sqrt{\pi}} \sin[k(x + a) + \delta_k] & x > 0 \end{cases} \tag{2}$$

where the phase shift δ_k is given by [13]

$$\delta_k = -ka + \tan^{-1}\left(\frac{ka}{G + ka\cot ka}\right) \qquad G = ga. \tag{3}$$

The quantity G is a dimensionless constant. It is understood that the wavefunction always vanishes for $x \leqslant -a$. We normalize the stationary wavefunctions in the usual manner [14] as

$$\int_{-a}^{\infty} \phi_k(x)\phi_{k'}(x)\,\mathrm{d}x = \delta(k - k'). \tag{4}$$

For the strength of the δ-function potential at $x = 0$, Winter took $G = 6$ and 20. We, however, take $G = 6$ and 100. In this way we can see the contrast between fast and slow decay processes more clearly. The phase shift δ_k may go through $\pi/2$ (mod π) upwards for a certain value of k or E. This means that there is a resonance at that energy. Such a resonance corresponds to one of the poles of the integrand that we examine shortly. When $G = 6$ there is only one resonance due to a pole labelled by $\nu = 1$. When $G = 100$ there are 15 resonances with $\nu = 1, 2, \ldots, 15$.

We are interested in the time-dependent wavefunction that is subject to the initial condition

$$\psi(x, 0) = \begin{cases} \sqrt{2/a}\sin(n\pi x/a) & -a < x < 0 \\ 0 & 0 < x \end{cases} \tag{5}$$

where $n = 1, 2, \ldots$. In the illustrations that follow we take $n = 1$. There is no particular difficulty in taking $n = 2, 3, \ldots$, or a combination of components with different values of n. The function $\psi(x, 0)$ is normalized. The expectation value of the energy in this state is $(n\pi/a)^2/2m$. The wavefunction $\psi(x, t)$ at a later time t can be expressed as a superposition of stationary states. Winter writes it as

$$\psi(x, t) = \int_0^{\infty} f(q)\,\mathrm{d}q \tag{6}$$

where

$$f(q) = 2n\sqrt{\frac{2}{a}}\frac{\mathrm{e}^{-\mathrm{i}q^2T} q \sin q[q\sin q(\xi + 1) + G\theta(x)\sin q\sin q\xi]}{(q^2 - n^2\pi^2)(q^2 + Gq\sin 2q + G^2\sin^2 q)}. \tag{7}$$

We have used dimensionless variables defined by

$$q = ka \qquad T = t/(2ma^2) \qquad \xi = x/a. \tag{8}$$

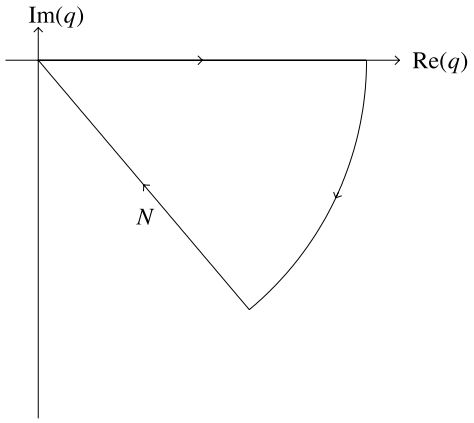

Figure 1. The integration contour of equation (9) in the complex q-space.

The ξ is Winter's l. Petzold obtained a different but equivalent expression for $\psi(x,t)$ by means of the Laplace transform [8]. García-Calderón *et al* [10–12] also used Laplace transforms. We find Winter's formula somewhat simpler.

To evaluate the wavefunction $\psi(x,t)$ of equation (6) is not easy. To our knowledge such a wavefunction has not been obtained except for the special case of $x = 0$ which was done by Winter [9]. He calculated $\psi(0,t)$ and the probability current $j(0,t)$ at the barrier and examined the nature of the decaying system. We are interested in $\psi(x,t)$ and $j(x,t)$ for $x \neq 0$, in particular, for large values of x. Following Winter we try to evaluate the integral of equation (6) by using a closed contour in the complex plane, as shown schematically in figure 1. If we replace q with $z = s\mathrm{e}^{\mathrm{i}\theta}$, the factor $\mathrm{e}^{-\mathrm{i}q^2T}$ in equation (7) becomes $\mathrm{e}^{-\mathrm{i}s^2T\cos 2\theta}\mathrm{e}^{s^2T\sin 2\theta}$. This factor tends to zero as $s \to \infty$ if $0 > \theta > -\pi/2$. The integral along the arc becomes negligible in this limit. Therefore, the integral for the wavefunction can be reduced to the integral along the line N and contributions from the poles enclosed by the contour,

$$\psi(x,t) = -\left[\int_N f(z)\,\mathrm{d}z + 2\pi\mathrm{i}\sum(\text{residues})\right]. \tag{9}$$

The factor $(z^2 - n^2\pi^2)$ of the denominator of $f(z)$ does not give rise to any poles. This is because of the $\sin z$ of the numerator. The poles of $f(z)$ are determined by

$$z^2 + Gz\sin 2z + G^2\sin^2 z = 0. \tag{10}$$

If $G \gg 1$, $\sin z \approx 0$ and hence $z \approx \nu\pi$ where $\nu = 1, 2, \ldots$, or more accurately

$$z_\nu \approx \nu\pi\left(1 - \frac{1}{G} + \frac{1}{G^2} \pm \frac{\mathrm{i}\nu\pi}{G^2}\right) \tag{11}$$

where we have ignored terms like $1/G^3$, etc. Only the poles with a negative imaginary part lie inside the contour. The energy E_ν and width Γ_ν of the resonances are determined by ${z_\nu}^2/2ma^2 = E_\nu - \mathrm{i}\Gamma_\nu/2$. If $G \gg 1$, we obtain

$$E_\nu \approx \frac{1}{2m}\left(\frac{\nu\pi}{a}\right)^2\left(1 - \frac{2}{G} + \frac{3}{G^2}\right) \qquad \Gamma_\nu \approx \frac{1}{2m}\frac{4(\nu\pi)^3}{G^2a^2}. \tag{12}$$

Among the poles, the z_ν with $\nu = n$ contributes dominantly to the integral. If we single out this pole contribution, we obtain

$$\psi(x,t) \approx \begin{cases} \sqrt{\dfrac{2}{a}}\,\mathrm{e}^{-\mathrm{i}E_n - \frac{1}{2}\Gamma_n t}\left[\sin\dfrac{z_n x}{a} - \dfrac{z_n(x+a)}{Ga}\cos\dfrac{z_n x}{a}\right] & -a < x < 0 \\ \sqrt{\dfrac{2}{a}}\,\mathrm{e}^{-\mathrm{i}E_n - \frac{1}{2}\Gamma_n t}\left(-\dfrac{z_n}{G}\right)\mathrm{e}^{\mathrm{i}z_n x/a} & x > 0 \end{cases} \tag{13}$$

which is essentially the Gamow wavefunction for the δ-function potential model. The amplitude of this $\psi(x,t)$ decays exponentially in time. Outside the barrier, the wavefunction is an outgoing wave. For a given t the amplitude grows exponentially as x increases. This is because of the imaginary part of z_n. This wavefunction is not normalizable in the usual manner over the entire coordinate space. Other potential models yield Gamow wavefunctions with similar properties [4].

For $G = 6$, expansions like equations (11) and (12) are not very accurate. A more accurate estimate gives $\Gamma_\nu/E_\nu \approx 0.13$ which is not very small. For $G = 100$, the expansions in $1/G$ works well. The resonances are sharp as can be seen from $\Gamma_\nu/E_\nu \approx 4\nu\pi/G^2 \approx (1.3\times10^{-3})\nu$. The width increases as ν increases. In extending Winter's calculation for the wavefunction, we have to determine the poles with great accuracy. This can be done as follows. Taking the real and imaginary parts of equation (10) we obtain two coupled equations. The problem is then reduced to finding intersections of two curves in the complex z-plane [15]. Starting with the approximate solution (11), we can solve the coupled equations by iteration to any desired accuracy.

For the line N it is convenient to choose $\theta = -\pi/4$ so that $\mathrm{e}^{-\mathrm{i}z^2T} = \mathrm{e}^{-2s^2T}$. This factor appears to make the integrand decay rapidly for finite t. However, the integrand also contains the factors $\mathrm{e}^{\xi s}$, $\cos\xi s$, $\sin\xi s$, as well as a factor that varies slowly with s and falls off as $1/s^2$ for large s. The integral cannot be done analytically. It converges but its numerical integration provides a challenge. For large values of x, the wavefunction, as we will show in the next section, is very small. However, when $T = 2$ and $\xi = x/a = 50$, for example, $\mathrm{e}^{-2Ts^2+\xi s}$ has a maximum value of 5×10^{67}. With values of the integrand this large, numerical quadratures will not be able to give results of small values of the integral because of the limited precision normally provided by computers. For values of $\xi = x/a$ up to about 20 (when $T = 2$), any reasonably sophisticated quadrature or Fourier transform routines give reliable results. But it is difficult to go further. It should be noted that to obtain a reliable wavefunction, the contributions due to the poles, which blow up at large x, must be combined with the contribution due to the line integral along N.

In figure 2, we show the modulus of the wavefunction $|\psi(x,t)|$ for $G = 6$ that we obtained by using equations (6) and (9). In this figure and in dealing with numerical values in the following, we take units such that $a = 1$ and $2m = 1$ as we said below equation (1). Then we have $\xi = x$ and $T = t$. The wavefunction of figure 2 is for $t = 2$. It is not reliable beyond $x \approx 20$. Figure 3 shows $|\psi(x,t)|$ for $G = 6$ and $t = 2$ that we obtained by solving the time-dependent Schrödinger equation numerically as we will explain in the next section. This wavefunction agrees very well with that of figure 2 up to $x \approx 20$.

One of the very interesting features that Winter obtained is the oscillations in the probability current, for $G = 6$ at $x = 0$ around $t = 10$. The current is negative at times. He found similar oscillations for $G = 20$. In figure 4 we reproduce Winter's result for $t = 0$–12, and in figures 5 and 6 we obtain the probability current profile for the time intervals from $t = 7$–15 when $x = 3$ and 10. Surprisingly, the oscillations not only persist but their amplitudes (and their maximum negative values) increase by orders of magnitude as x increases. We also confirm Winter's results using the numerical method described in section 3. We are therefore convinced that the

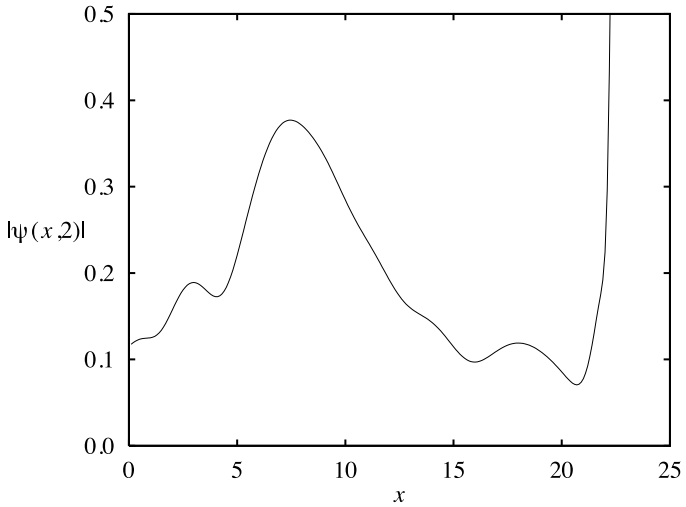

Figure 2. The modulus of the wavefunction $|\psi(x,t)|$ for $G = 6$ and $t = 2$, obtained by using equation (6). Units are such that $\hbar = 1$, $2m = 1$ and $a = 1$. The wavefunction is reliable up to $x \approx 20$, beyond which the results are marred by huge rounding errors.

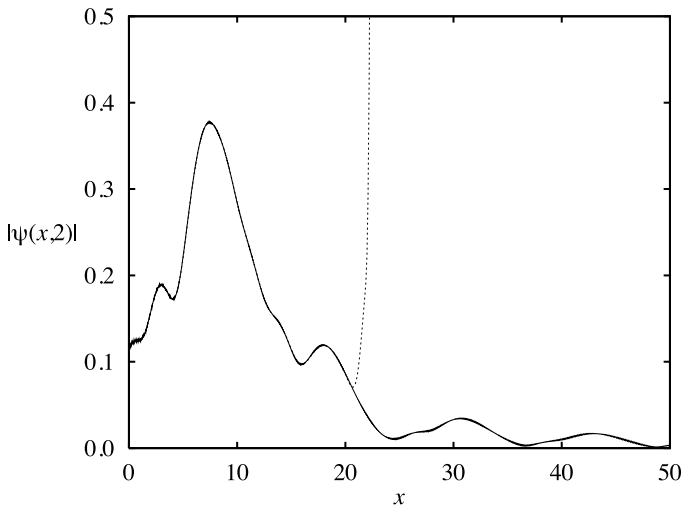

Figure 3. The modulus of the wavefunction $|\psi(x,t)|$ for $G = 6$ and $t = 2$, obtained by solving the time-dependent Schrödinger equation numerically (section 3). The units are the same as in figure 2. The dotted curve is that of figure 2. The two curves overlap for $x < 20$.

negative currents are physical and not due to numerical uncertainties. We return to this point in section 3 where we find out more about the details of the wavefunction.

3. Integration of the time-dependent Schrödinger equation

In order to obtain the wavefunction of the decaying system let us solve a difference-equation version of the time-dependent Schrödinger equation. Such calculations have been done for scattering systems [16, 17], but not for a decaying state. We assume that space and time are

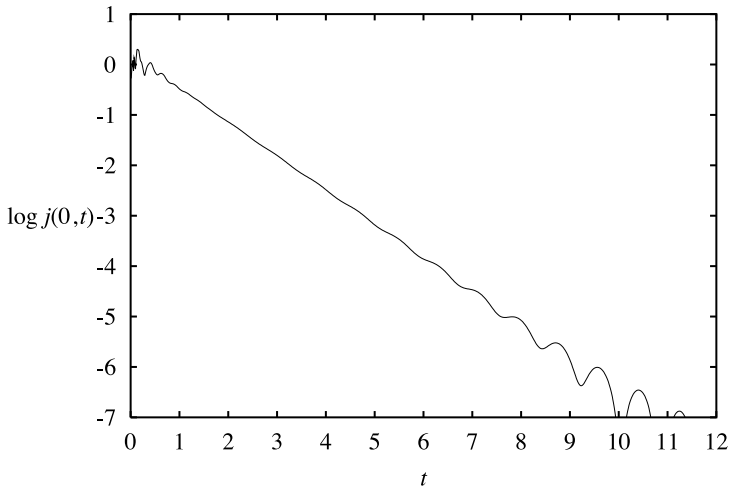

Figure 4. The current at the barrier $x = 0$, for $G = 6$, from $t = 0$–12. This was obtained by Winter [8]. The units are the same as in figure 2.

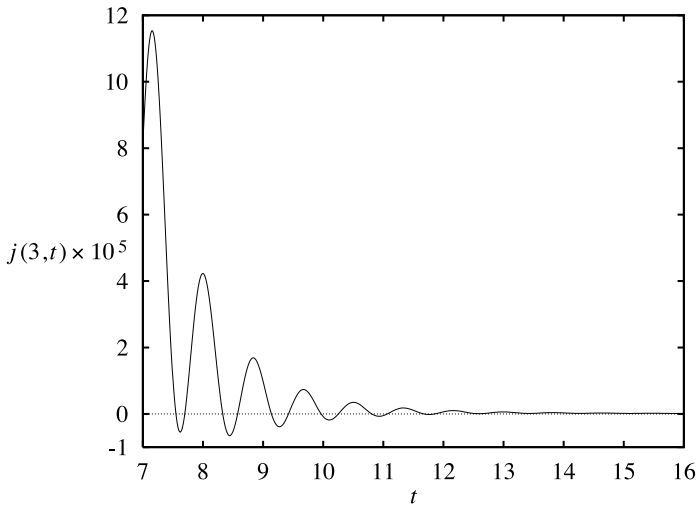

Figure 5. The current at $x = 3$ for $G = 6$ from $t = 7$–16. The units are the same as in figure 2.

discretized with small intervals of Δx and Δt, and $\psi(x, t + \Delta)$ and $\psi(x, t)$ are related by

$$\psi(x, t + \Delta t) = \frac{1 - \frac{\mathrm{i}}{2} H \Delta t}{1 + \frac{\mathrm{i}}{2} H \Delta t} \psi(x, t). \tag{14}$$

Here H is the Hamiltonian which we interpret as

$$H = -\frac{1}{2m} D^2 + V(x) \tag{15}$$

where D^2 is the operator such that

$$D^2 \psi(x, t) = \frac{1}{(\Delta x)^2} [\psi(x + \Delta x, t) - 2\psi(x, t) + \psi(x - \Delta x, t)]. \tag{16}$$

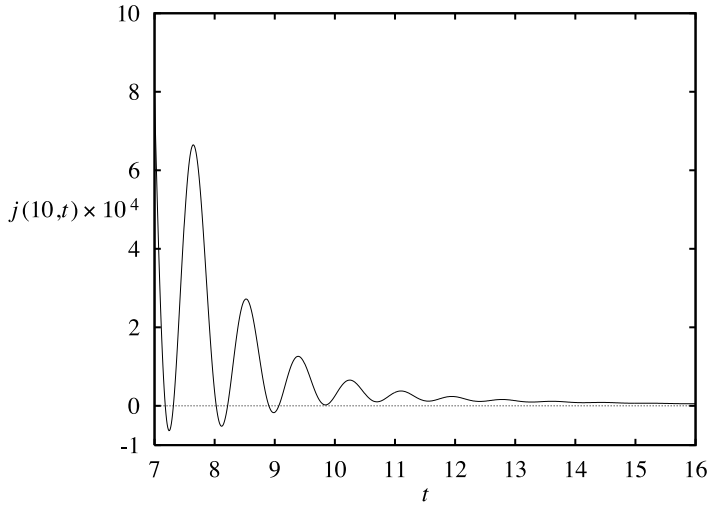

Figure 6. The current at $x = 10$ for $G = 6$ from $t = 7$–16. The units are the same as in figure 2.

The wavefunction can be expressed as an array of $\psi_{i,n} \equiv \psi(x_i, t)$, where x_i are the discretized points with equal interval Δx. Then equation (14) can be put into a form of a system of linear equations for $\psi_{i,n+1} = \psi(x_i, t + \Delta t)$. We do this by operating $1 + \frac{\mathrm{i}}{2} H \Delta t$ on equation (14) from the left.

Transformation (14) is unitary and consequently the normalization of the wavefunction in the sense of $\sum_i |\psi(x_i, t)|^2 \Delta x = 1$ is exactly maintained. Let us add that if one uses Simpson's rule rather than the trapezoidal summation formula, the normalization may not be exactly maintained. Furthermore, the expectation value of the Hamiltonian,

$$\langle H \rangle = \sum_i \psi^*(x_i, t)(D^2 + V)\psi(x_i, t)\Delta x \tag{17}$$

remains also constant for all t. This is so even if Δt and Δx are not small. We have also verified that the discretized version of the Ehrenfest relation $\langle p \rangle = m\, \mathrm{d}\langle x \rangle / \mathrm{d}t$ is valid for sufficiently small Δx and Δt. For the initial wavefunction we take the discretized version of $\psi(x, 0)$ of equation (5) with the same factor of $\sqrt{2/a}$. It is exactly normalized as $\sum_i |\psi(x_i, 0)|^2 \Delta x = 1$. As is the case with wavepacket scattering [16] a higher-order formula of D^2 is not required to give sufficiently accurate results.

For Δx and Δt in numerical illustrations, we take $\Delta x = 0.01$ and $\Delta t = 0.005$. We replace the δ-function potential at $x = 0$ with a square barrier of width Δx and height $G/\Delta x$. Effects of finite meshes are almost invisible in the figures that we show. For t we start with $t = 0$ and go up to $t \approx 50$. In order to have a feel for the space-time scale, let us note that the radius of the 'model nucleus' is $a = 1$, the decay half-life is $\tau_{1/2} = \ln 2/\Gamma \approx 1.08$ for $G = 6$ and $\tau_{1/2} \approx 56$ for $G = 100$. For the range of x, we take $[-1, 999]$. The $x_{max} = 999$ is large enough such that its finiteness has no discernible effect on our numerical solution.

We have already shown $|\psi(x, t)|$ for $G = 6$ and $t = 2$ in figure 3. Figure 7 shows $|\psi(x, t)|$ for $G = 6$, $t = 5$, 10, 15, 20, 25, and 30. Figure 8 shows the same quantities as those of figure 7, except that $G = 100$ this time. In figure 8 we can clearly see a wavefront structure of the wavefunction. The wavefront proceeds with speed $v = \pi$. We can also see small crests proceeding with greater speeds of 2π and 3π. These small crests can be understood as follows. When the initial wavefunction $\psi(x, 0)$ is written as a superposition of stationary states $\phi_k(x)$, in addition to the main contribution from the resonance of $n = 1$, higher resonances of

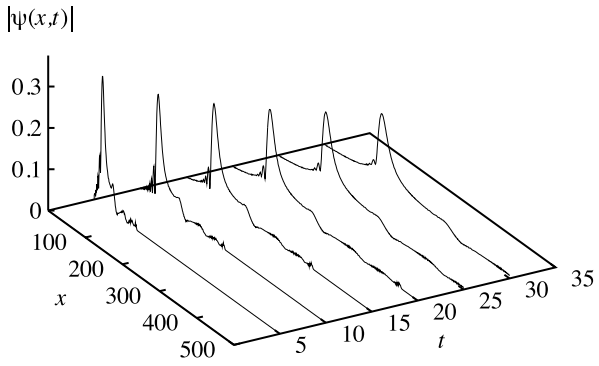

Figure 7. The modulus of the wavefunction $|\psi(x,t)|$ for $G = 6$ and $t = 0$, 5, 10, 15, 20, 25, and 30. The units are the same as in figure 2.

$n = 2, 3, \ldots$ also contribute. In the case of $G = 6$ the structure of the wavefunction is more complicated.

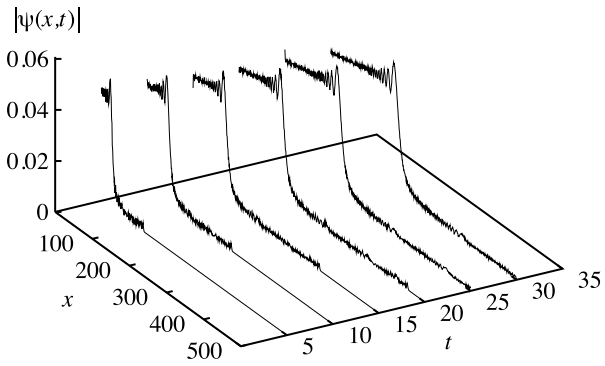

Figure 8. The modulus of the wavefunction $|\psi(x,t)|$ for $G = 100$ and $t = 0$, 5, 10, 15, 20, 25, and 30. The units are the same as in figure 2.

In figures 4–6 we showed the current as a function of time for $G = 6$ at $x = 0$, 3 and 10. We noted that the amplitude of the fluctuations is larger for larger values of x. This can be related to the wavefunction shown in figure 7. Note that the major peak at $x \approx 50$ in the curve for $t = 10$ is followed by many small peaks with about the same intervals. Every time such a peak passes through a point, the current at that point increases. The height of the peak is larger for larger x. Figure 7, by itself, does not show that the current is negative at certain points. This could be done by comparing the wavefunction at t and the one at a slightly different time.

To shed further light on the current fluctuations, we plot the current at $t = 8.25$ as a function of x in figure 9. The curve for the current in the main part of the graph is calculated using the numerical solution of the Schrödinger equation. The local fluctuations of the current are due to the fact that x has been discretized with a finite interval Δx. We note that the current follows the probability density (dotted curve), i.e., they have local extrema at the same values of x. The inset shows the analytical calculation (of section 2) of the current for smaller values of x than those of the main peak. This shows that the current is negative at its minimum values, but only slightly so, compared with the overall amplitude of the current. The fact that the current has negative values locally does not contradict the idea that the overall wave pattern

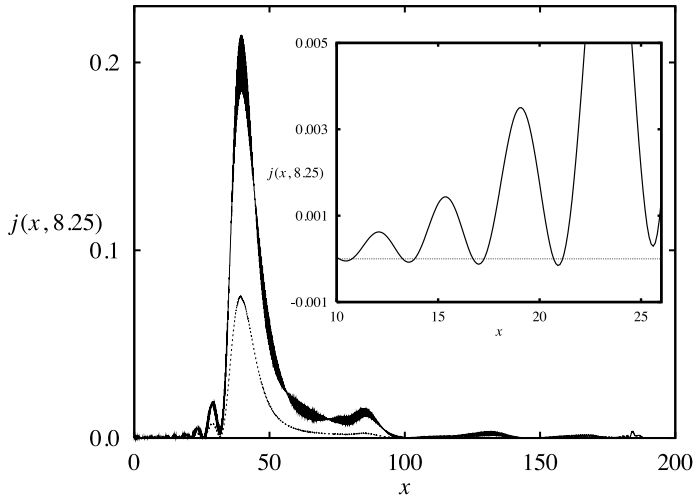

Figure 9. The current density $j(x, t = 8.25)$ as a function of x is shown as the solid curve, when $G = 6$. The dotted curve is the probability density $|\psi(x, 8.25)|^2$. The inset gives an expanded view of the current calculated by the method of section 2 in the region where it has negative minima.

is travelling outward. The negative currents are very small and occur where the amplitude of the wave is already a small fraction of the main peak and at times of the order of ten half-lives of the decaying system. See the appendix in this connection. The amount by which the current becomes negative increases as x increases up to the second last local minimum before the main peak of the wave pattern. Let us add that the current exhibits fluctuations also at very short times. This is related to the part of the wavefunction that propagates ahead of the main peak.

All these calculations can be repeated using a Gaussian potential in place of the δ-function potential. We find very little difference in the results if a Gaussian with a width of 0.1 at the 'nuclear' boundary is used starting with the same initial state. This more realistic model of the Coulomb barrier does not affect the features discussed in this paper.

4. Approximate wavefunction for $x > 0$

Since we wish to eventually obtain a wavefunction for the decaying system that can be used in the quantum mechanical calculation of the ionization probability due to the emitted α particle, we propose an approximate form of the wavefunction for $x > 0$. Such a wavefunction is needed since it is difficult to integrate numerically the time-dependent Schrödinger equation for the α particle to distances comparable to the size of the atom. We are particularly interested in such a wavefunction appropriate to a long-lived α emitter.

Let us consider a situation such that the particle inside the potential barrier is in a very sharp resonance state, the decay rate is very small and the exponential decay law holds. We assume that the probability distribution flows outwards with a constant speed v, which is also the speed of the emerging α particle. Then the probability density $\rho(0, t)$ and current $j(0, t)$ just outside the barrier are related by $j(0, t) = v\rho(0, t)$. The current is equal to $-(\mathrm{d}/\mathrm{d}t)\mathrm{e}^{-\Gamma t} = \Gamma \mathrm{e}^{-\Gamma t}$, which leads to

$$\rho(0, t) = \frac{\Gamma}{v}\mathrm{e}^{-\Gamma t}\theta(t) \tag{18}$$

where $\theta(t)$ ensures that there was no leakage of the probability before $t = 0$. If we assume

that the probability flows out uniformly with speed v, we obtain

$$\rho(x,t) = \frac{\Gamma}{v} \mathrm{e}^{-\Gamma(t-\frac{x}{v})} \theta\left(t - \frac{x}{v}\right) \tag{19}$$

where it is understood that $x > 0$. This $\rho(x,t)$ is normalized as $\int_0^\infty \rho(x,t)\,\mathrm{d}x = 1 - \mathrm{e}^{-\Gamma t}$. If there are a large number, N_0, of decaying samples at $t = 0$ and all at $x = 0$ and if one counts the number of emitted particles detected at a certain position x from time t to $t + \Delta t$, one will find it to be $N_0 \rho(x,t) v \Delta t$.

For the wavefunction outside the barrier it would be reasonable to assume, apart from a possible additional phase factor,

$$\phi(x,t) = \sqrt{\rho(x,t)}\mathrm{e}^{-\mathrm{i}Et}\mathrm{e}^{\mathrm{i}kx} \tag{20}$$

where $E = k^2/2m$ and $k = mv$. This wavefunction is normalized to $1 - \mathrm{e}^{-\Gamma t}$ and conforms to $j(0,t) = \Gamma \mathrm{e}^{-\Gamma t}$. By substituting this wavefunction into the Schrödinger equation $\mathrm{i}\partial\phi/\partial t = -(1/2m)\partial^2\phi/\partial x^2$ for $0 < x < vt$, we find that we need additional phase factors. In this way we arrive at

$$\phi(x,t) = \sqrt{\frac{\Gamma}{v}}\mathrm{e}^{\mathrm{i}\gamma}\mathrm{e}^{-\frac{\Gamma}{2}(t-\frac{x}{v})}\mathrm{e}^{-\mathrm{i}[E-\frac{1}{2m}(\frac{\Gamma}{2v})^2]t}\mathrm{e}^{\mathrm{i}kx}\theta\left(t - \frac{x}{v}\right) \tag{21}$$

where the constant phase factor $\mathrm{e}^{\mathrm{i}\gamma}$ is related to the choice of the initial wavefunction. Keeping one further term of the expansion in $1/G$ of the approximation of Γ in equation (12), we obtain the expressions for v and Γ which we used to evaluate the wavefunctions shown in figure 10, i.e.,

$$v \approx 2\pi\sqrt{1 - 2/G} \tag{22}$$

and

$$\Gamma \approx \frac{4\pi^3}{G^2}\left(1 - \frac{1}{G}\right) \tag{23}$$

where $a = 2m = 1$. It should be noted that equation (21) is an exact solution of the time-dependent Schrödinger equation for $0 < x < vt$.

Figure 10 compares for $G = 100$, the modulus of the approximate wavefunction and the one obtained by solving the time-dependent Schrödinger equation numerically. The approximate wavefunction works well for $G = 100$. However, it does not give a good representation of the wavefunction for $G = 6$. Recall that for $G = 6$, $\Gamma/E \approx 0.13$ which is not very small. It is clear that we cannot assume a uniform speed v in this case. In contrast to this, for $G = 100$, $\Gamma/E \approx 1.3 \times 10^{-3}$. As we point out in section 5, the value of Γ/E is much smaller in the actual α-decay processes. The wavefunction (21) will work even better in such situations.

Figure 10 shows only the modulus of the wavefunction. For the phase of the wavefunction, if we set $\mathrm{e}^{\mathrm{i}\gamma} = -1$, the phase of the approximate wavefunction for $G = 100$ becomes virtually indistinguishable from that of the wavefunction obtained by solving the time-dependent Schrödinger equation. The reason for this choice of γ is the following. The $\psi(x,0)$ is negative just inside the barrier. When it leaks out through the barrier the wavefunction remembers its sign, that is, $\mathrm{Re}\,\psi(\Delta x, \Delta t) < 0$.

We have obtained the approximate wavefunction for outside of the potential barrier. For the inside, a first approximation is

$$\phi(x,t) = \mathrm{e}^{-\mathrm{i}(E-\frac{i}{2}\Gamma)t}\psi(x,0) \qquad \text{for} \quad -a < x < 0 \tag{24}$$

where $\psi(x,0)$ is that of equation (5). We have confirmed that this is a good approximation when $G \gg 1$. This $\phi(x,t)$ for the inside together with that of equation (21) for the outside

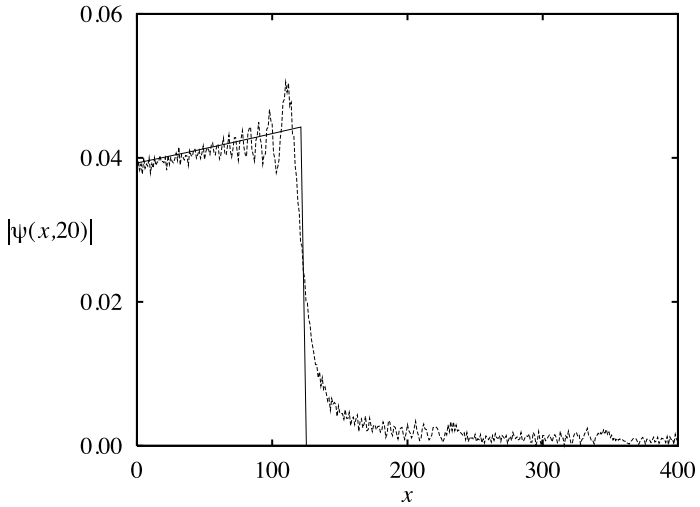

Figure 10. The absolute value of the approximate wavefunction $\phi(x, t)$ of equation (20) for $G = 100$ at $t = 20$ plotted as a solid line. The modulus of the actual wavefunction $\psi(x, t)$ as one of the curves in figure 8 is plotted as the dashed curve.

is correctly normalized to unity. The $\phi(x, t)$ of equation (24), however, vanishes at $x = 0$. Therefore, there is a slight mismatch at $x = 0$ between the inside and outside parts of this wavefunction.

5. Conclusion and discussion

We have examined a one-dimensional model that simulates, e.g., the α-decay process. A particle is initially confined within a 'nucleus' and begins to leak out at $t = 0$ tunnelling through a potential barrier. We were interested in obtaining the wavefunction of the model at all distances. We first attempted to extend Winter's calculation for the wavefunction. We were only able to do so up to a certain distance from the 'nucleus'. We examined the current outside the potential barrier. We found that the fluctuations of the current that Winter discovered become much larger as the distance from the potential barrier increases. These fluctuations can be understood in terms of the fluctuations of the wavefunction preceding and following the main peak. We then obtained the time-dependent wavefunction $\psi(x, t)$ in the entire space by solving the time-dependent Schrödinger equation numerically. As far as we know this is the first time that such a wavefunction has been obtained explicitly. When the potential barrier is very strong and the decay rate is very low, the $\psi(x, t)$ obtains a simple structure. It can be well represented by the approximate wavefunction $\phi(x, t)$ which we obtained in a heuristic manner. Unlike the commonly used Gamow wavefunction, this wavefunction (and of course the solution of the time-dependent Schrödinger equation) is normalized in the usual manner. Our approximate wavefunction is expected to be useful in quantum mechanical calculations of the atomic ionization process caused by nuclear α decay.

For the strength of the potential barrier that controls the decay rate, we considered two cases, $G = 6$ and 100. For the main resonance (of $n = 1$) that is involved, $\Gamma/E \approx 0.13$ for $G = 6$ whereas $\Gamma/E \approx 1.3 \times 10^{-3}$ for $G = 100$. These choices of the value of G represent two typical situations: the resonance is rather broad in one and is very sharp in the other. In the actual α-decay processes, the ratio Γ/E is much, much smaller. As an example let us

consider Po^{212} as the parent nucleus. Its decay rate is the fastest among the usually listed α-decay examples, e.g., see [18]. The energy of the emitted α particle is $E = 8.95$ MeV and $\Gamma = 2.31 \times 10^6\ s^{-1}$. This means the dimensionless ratio of $\Gamma/E = 1.70 \times 10^{-16}$. Note that in natural units ($c = 1, \hbar = 1$), $1\ s^{-1} = 6.58 \times 10^{-22}$ MeV. The ratio can be reproduced by our model with $G = 3.7 \times 10^8$. When G is this large, the wavefunction of equation (21) works extremely well. It will be very useful as an approximate wavefunction for the α particle in examining atomic ionization caused by α decay.

The reason why we took small values of G, which are unrealistic for α decay, in our numerical illustrations is the following. If G is very large and accordingly the decay is very slow, we have to integrate the Schrödinger equation to a very large value of t before we can see anything interesting. This is technically difficult. The quantity Γ which is proportional to the reciprocal of the half-life, however, is a power series in $1/G$ starting with $1/G^2$. Thus for very large G, the half-life scales as G^2. We therefore believe that $G = 100$ is sufficiently large to illustrate the essential features of cases of very strong G.

Acknowledgments

We would like to thank Dr David Kiang for many inspiring discussions on the subject over the years. We also thank Dr Fred Kus for helpful suggestions regarding some numerical aspects of the paper. This work was supported by the Natural Sciences and Engineering Research Council of Canada.

Appendix

In this appendix we illustrate a situation such that, even if the expectation value of the momentum is positive, the current density can be locally negative. This phenomenon was first observed in connection with decay problem by Winter [9] and is corroborated by the results of this paper.

Let us start with a free Gaussian wavepacket with its centre at rest at the origin. Its wavefunction is [19]

$$\phi_0(x,t) = (2\pi)^{-1/4}\left(\lambda + \frac{\mathrm{i}t}{2m\lambda}\right)^{-1} \exp\left(\frac{-x^2}{4\lambda^2 + 2\mathrm{i}t/m}\right) \tag{A.1}$$

where $(\Delta x)_{t=0} = \lambda$. The current density is given by

$$j_0(x,t) = \frac{xt}{m^2\lambda^4 + t^2}|\phi_0(x,t)|^2. \tag{A.2}$$

The expectation value of $j_0(x,t)$ is zero.

Next we let the wavepacket move with a constant speed $v > 0$. The wavefunction and current density become

$$\phi(x,t) = \phi_0(x - vt, t)\mathrm{e}^{\mathrm{i}(mvx - \frac{1}{2}mv^2t)} \tag{A.3}$$

$$j(x,t) = v|\phi(x,t)|^2 + j_0(x - vt, t). \tag{A.4}$$

In (A.4) the second term can be negative. The first term, however, normally dominates so that $j(x,t)$ is positive.

A more interesting situation obtains if we assume that $\psi(x,t)$ is a superposition of two wavepackets,

$$\psi(x,t) = c_1\psi_1(x,t) + c_2\psi_2(x,t) \tag{A.5}$$

$$\psi_1(x,t) = \phi(x - b, t) \qquad \psi_2(x,t) = \phi(x + b, t). \tag{A.6}$$

The two wavepackets are separated by distance $2b$. They both move with speed v. For simplicity let us assume that c_1 and c_2 are both real and

$$|c_1 + c_2| \ll 1. \tag{A.7}$$

It then follows that $\psi(x,t)$ vanishes in the vicinity of the midpoint ($x = vt$) of the two wavepackets. The current density at $x = vt$ turns out to be

$$j(x = vt, t) = \left[(c_1 + c_2)^2 v - \frac{(c_1^2 - c_2^2)bt}{4m^2\lambda^4 + t^2}\right] |\psi(x,t)|^2. \tag{A.8}$$

If we put $c_1 = c + \epsilon$ and $c_2 = -c + \epsilon$ then $(c_1 + c_2)^2 = 4\epsilon^2$ and $c_1^2 - c_2^2 = 4c\epsilon$. If $|\epsilon/c| \ll 1$, then the second term in the square brackets of (A.8) can become more important than the first, and $j(x,t)$ can become negative. Note that the negative current density occurs when the probability density almost vanishes.

We have chosen c_1 and c_2 such that they are approximately equal in magnitude. If we choose c_1 larger than c_2 in magnitude, the point at which $\psi(x,t)$ vanishes is shifted towards the second wavepacket. In the vicinity of that point, $j(x,t)$ can become negative.

References

[1] Gamow G 1928 *Z. Phys.* **51** 204
Gamow G 1928 *Z. Phys.* **52** 510
Gamow G and Critchfield C L 1949 *Theory of Atomic Nucleus and Nuclear Energy-Sources* (Oxford: Clarendon) ch 6

[2] Condon E U and Gurney R W 1928 *Nature* **112** 439
Condon E U and Gurney R W 1929 *Phys. Rev.* **33** 127

[3] Weinberg A M 1952 *Phys. Rev.* **20** 401
Hokkyo N 1965 *Prog. Theor. Phys.* **33** 1116
García-Calderón G and Peierls R 1976 *Nucl. Phys.* A **265** 443

[4] Bohm A, Gadella M and Mainland G B 1989 *Am. J. Phys.* **57** 1103

[5] Migdal A 1941 *J. Phys. (USSR)* **4** 449

[6] Levinger J S 1953 *Phys. Rev.* **90** 11

[7] Révai J and Nogami Y 1992 *Few-Body Syst.* **13** 75

[8] Petzold J 1959 *Z. Phys.* **155** 422

[9] Winter R G 1961 *Phys. Rev.* **123** 1503

[10] García-Calderón G 1992 *Symmetries in Physics* ed A Frank and K B Wolf (New York: Springer) p 252

[11] García-Calderón G, Loyola G and Moshinsky M 1992 *Symmetries in Physics* ed A Frank and K B Wolf (New York: Springer) p 273

[12] García-Calderón G, Mateos J L and Moshinsky M 1993 *Rev. Mex. Fis.* (Suppl 2) **39** 76
García-Calderón G, Mateos J L and Moshinsky M 1995 *Phys. Rev. Lett.* **74** 337
García-Calderón G, Mateos J L and Moshinsky M 1996 *Ann. Phys., NY* **249** 430

[13] Massmann H 1985 *Am. J. Phys* **53** 679

[14] Brownstein K R 1975 *Am. J. Phys.* **43** 173

[15] Onley D and Kumar A 1991 *Am. J. Phys.* **59** 562

[16] Goldberg A, Schey H M and Schwartz J L 1967 *Am. J. Phys.* **35** 177

[17] Bonche P, Koonin S and Negele J W 1976 *Phys. Rev.* C **13** 1226
Press W H, Flannery B P, Teukolsky S A and Vetterling W T 1988 *Numerical Recipes in C* (Cambridge: Cambridge University Press) pp 661–3

[18] French A P and Taylor E F 1978 *An Introduction to Quantum Mechanics* (New York: W W Norton and Co Inc) p 407

[19] Schiff L I 1968 *Quantum Mechanics* 3rd edn (New York: McGraw-Hill) ch 3